Subpromille Measurements and Calculations of CO (3–0) Overtone Line Intensities

Katarzyna Bielska[1], Aleksandra A. Kyuberis[2], Zachary D. Reed[3], Gang Li[4], Agata Cygan[1],
Roman Ciuryło[1], Erin M. Adkins[3], Lorenzo Lodi[5], Nikolay F. Zobov[5], Volker Ebert[4], Daniel Lisak[1],
Joseph T. Hodges[3], Jonathan Tennyson[5,*], and Oleg L. Polyansky[5]

[1]Institute of Physics, Faculty of Physics, Astronomy and Informatics, Nicolaus Copernicus University in Toruń,
Grudziadzka 5, 87-100 Torun, Poland
[2]Van Swinderen Institute for Particle Physics and Gravity, University of Groningen,
Nijenborgh 4, 9747AG Groningen, The Netherlands
[3]Chemical Sciences Division, National Institute of Standards and Technology, Gaithersburg, Maryland 20899, USA
[4]PTB (Physikalisch-Technische Bundesanstalt), Bundesallee 100, 38116 Braunschweig, Germany
[5]Department of Physics and Astronomy, University College London,
Gower Street, London WC1E 6BT, United Kingdom

Intensities of lines in the near-infrared second overtone band (3–0) of $^{12}C^{16}O$ are measured and calculated to an unprecedented degree of precision and accuracy. Agreement between theory and experiment to better than 1‰ is demonstrated by results from two laboratories involving two independent absorption- and dispersion-based cavity-enhanced techniques. Similarly, independent Fourier transform spectroscopy measurements of stronger lines in this band yield mutual agreement and consistency with theory at the 1‰ level. This set of highly accurate intensities can provide an intrinsic reference for reducing biases in future measurements of spectroscopic peak areas.

Spectroscopic measurements of transition frequencies (line positions) of gaseous molecules provide some of the most accurate measurements in the whole of science, with relative uncertainties as low as a few parts in 10^{12} [1]. Even standard laboratory setups can routinely provide line positions of rotation-vibrational lines in the infrared (ir), microwave, and optical region with relative uncertainties of a few parts in 10^8. The situation is very different for line intensities, for which the level of accuracy achievable by both experiments and theory is usually much lower, typically in the range 1–20%. Nevertheless, over the past 20 years or so it has become possible in some cases to obtain line intensities with a relative standard uncertainty less than 1% [2]. More recently, intensity measurements with combined uncertainties at the promille (1‰) level have been realized [3–6]. Such an accuracy is required for several applications, including detailed observations of the various constituents of the Earth's atmosphere, as well as analyses of the atmospheres of celestial bodies such as other Solar System planets, exoplanets, and cool dwarf stars. Highly accurate line intensities might also become useful for metrological purposes—for example, for new standards of temperature [7] and pressure [8,9], although the accuracy requirements are 1 to 2 orders of magnitude higher than presently possible. Nevertheless, absolute optical measurements of isotopic composition based on line intensities having uncertainties at the promille level [10] have recently been shown to be competitive with traditional approaches based on high-precision isotope-ratio mass spectrometry of reference materials.

Agreement between experiment and theory for some CO_2 lines in the near-ir and ir regions to a level better than 3‰ was reported by some of us [11]. Key to the success of this Letter was collaboration between experiment and theory that allowed the *ab initio* theoretical model to provide CO_2 transition intensities for atmospheric studies [12].

This Letter constitutes a contribution toward the ambitious goal of reliably measuring and computing molecular line intensities to subpromille accuracy. To this end, we turn to the calculation and measurement of intensities in the (3–0) band of $^{12}C^{16}O$. Compared to CO_2, CO is more amenable to accurate theoretical calculations and far less susceptible to experimental complications caused by adsorption and desorption from the walls of sample cells. There are also fewer overlapping spectra from adjacent lines, including those of its other isotopologues. To reduce statistical and systematic measurement uncertainties, we included independently measured line intensities from three laboratories, in which each group had metrology-grade expertise in quantitative spectroscopy with traceability to the Système International (SI). This set of experiments involved different measurement techniques and different gas samples for each group. Except for one value from Ref. [3], measurements were arranged in a blind approach so that experimenters did not know each other's results before the final line intensity data were revealed.

After combining results from all laboratories and substantially different measurement techniques described below, the dynamic range of the line intensities is $\approx 1400:1$. In the remainder of this Letter, all reported intensities are compared to the present *ab initio* theoretical calculations and to literature values.

Seven lines, namely R23, R26, R27, R28, R29, P27, and P30, were independently measured at the Nicolaus Copernicus University (NCU) and at the National Institute of Standards and Technology (NIST) using two different laser-based techniques. Measurements at NCU were made using the recently developed cavity-mode dispersion spectroscopy (CMDS) technique [13], which involves mode-by-mode measurements of shifts (dispersion) in cavity-mode frequencies under steady state laser excitation for gas pressures between 0.4 and 13.1 kPa. Spectra at NIST were acquired using the comb-linked cavity ring-down spectroscopy (CRDS) technique [14,15]. These CRDS spectra were acquired using mode-by-mode measurements of the laser-pumped ring-down cavity decay rate for gas pressures between 8.7 and 26.6 kPa. Importantly, we note that, unlike CMDS, CRDS measures light absorption by the sample instead of sample dispersion. Both of these observables are proportional to line intensity and connected by the principle of causality through the real and imaginary components of the complex-valued resonant susceptibility of the absorber [16].

To provide more extensive coverage of the (3–0) CO band, another set of measurements for stronger lines (P22 to R22) in the same band was measured at a gas pressure of 10.2 kPa at Physikalische Technische Bundesanstalt (PTB) [17] using the Fourier-transform spectroscopy (FTS) technique. The implementation of FTS here involves an incoherent light source coupled into a scanning interferometer to produce an interferogram, from which the spectrum is obtained through Fourier transformation.

All lines were fit with the Hartmann-Tran profile [18] or limiting cases of this profile. These analyses included first-order line-mixing effects, and both NCU and NIST used multispectrum fitting approaches [19]. Full details regarding the experiments and theoretical analysis are available in the Supplemental Material (SM) [20]; the SM also provides sample figures illustrating the spectra. Each group independently identified and evaluated both systematic and statistical sources of measurement uncertainty. In summary, the maximum systematic uncertainty components among all experiments included pressure (0.7‰), temperature dependence of sample density and line intensity (0.9‰), sample isotopic composition and purity (0.4‰), and spectral modeling (1‰). The maximum component of the uncertainty driven by statistical variations in the measurements was 1.4‰. For the NIST measurements, the effect of digitizer nonlinearity was also included (0.2‰), whereas for the FTS measurements at PTB uncertainty in sample path length was 0.12‰. Adding all components in quadrature resulted in line- and institution-dependent relative combined standard uncertainties ranging from 1‰ to 1.2‰ for NCU, 0.9‰ to 1.8‰ for NIST, and an average value of 1.3‰ for PTB.

The accuracy of intensity calculations (both purely *ab initio* and semiempirical) is determined by the accuracy of the wave functions and dipole moment curve (DMC), where uncertainty of the wave functions is based on the potential energy curve and solution of the nuclear-motion Schrödinger equation. Here, we used an empirical potential energy curve from Coxon *et al.* [34], which reproduces the CO transition frequencies within experimental uncertainty. DMCs were computed *ab initio* using the electronic structure package MOLPRO[35] at the multireference configuration interaction level of theory with a Davidson correction $(+Q)$ and a relativistic correction using an aug-cc-pCV6Z basis set.

Figure 1 summarizes the present results in four panels that show relative differences in intensity, S, versus, m, where $m = -J$ (P-branch), $m = J + 1$ (R-branch), and J is the lower-state rotational quantum number. In Fig. 1(a), we present the high-J line intensities measured by NCU and NIST, relative to the present theoretical calculations. The standard deviation of the relative differences between the experimental and calculated intensities as well as the relative differences between the measured quantities themselves are around 1‰ (excluding the relatively weak P30 transition); see Table I. To consolidate the measured intensities, we also evaluated the weighted mean intensity, S_{av}, at each value of m. The relative difference, $(S_{av}/S_{UCL} - 1)$, averaged over the remaining six lines [see black triangles in Fig. 1(a)] gives a mean value of -0.2‰ with a standard deviation of 0.7‰. These results are consistent with the uncertainties in the NCU and NIST measurements.

Special attention should also be paid to the R23 line intensity for which three independent sets of measurements (two at NCU and one at NIST) were made. This line was first measured by the NCU group with the method described above [3] and a second time for the present study. We also note that the CMDS measurement technique at NCU was compared to an alternative technique based on cavity buildup dispersion spectroscopy [43]. In that experiment, the R23 peak area was measured by both techniques and yielded a difference of 0.3‰, which is consistent with the combined uncertainties in both measurements of spectroscopic area. In the present results, the weighted average of the experimental intensities for the R23 line differs from the theoretical value by 0.2‰, with an uncertainty of 0.5‰. Given that the theoretical calculations and measured intensities of the most accurately measured lines agree to within the estimated uncertainties, the demonstrated 0.5‰ agreement is unlikely to be fortuitous.

The FTS results from PTB for the stronger lines are given in Fig. 1(b) and a representative subset of these data
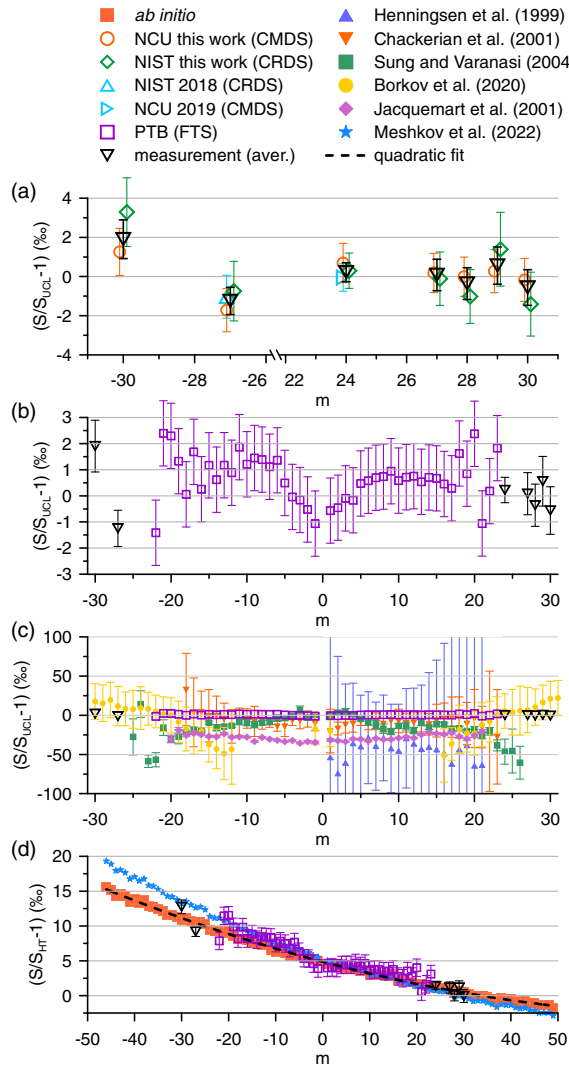
FIG. 1. Summary of present experimental and theoretical results for the (3–0) band of $^{12}C^{16}O$, and comparison to literature data. Panel (a): Comparison of NCU and NIST intensity measurements, S, for high-J lines, expressed as $(S/S_{UCL} - 1)$, where S_{UCL} are the present theoretical intensities. The black triangles represent weighted averages of the measurements. NCU 2019 indicates the measurement from Ref. [3] and NIST 2018 indicates a prior measurement conducted at NIST in 2018. Note the break in the x axis. Panel (b): Analogous comparison of low-J PTB intensity values and average high-J values from panel (a). Panel (c): m dependence of $(S/S_{UCL} - 1)$ where S corresponds to literature data [36–40] (closed symbols) and present measurements (open symbols). Note the extended range of the y-axis scale compared to the other panels. Panel (d): m dependence of $(S/S_{HT} - 1)$ where S corresponds to experimental (open symbols) and theoretical (orange squares) intensities from this work as well as semiempirical intensities from Ref. [41] (blue stars). S_{HT} are values from HITRAN 2020 [42] intensities scaled to 100% $^{12}C^{16}O$. The dashed line is a second-order polynomial fit of the ratio $(S_{UCL}/S_{HT} - 1)$ versus m. This function, $f(m) = a_0 + a_1 m + a_1 m^2$ provides a convenient mapping of the HITRAN 2020 intensities on to the present theoretical values. Here, $a_0 = 4.865‰$, $a_1 = -0.1789‰$, and $a_2 = 0.001020‰$. Note the differing x axes for the various panels.

is given in Table I; see SM for all data. In summary, the set of relative differences between the intensities measured by PTB and the theoretical predictions has a mean value of 0.7‰ with a standard deviation of 0.9‰. For the subset from $m = -10$ to 14 containing the strongest lines, the mean value is 0.4‰ and the standard deviation is 0.7‰, thus quantifying excellent agreement with the theory. Also shown in this figure are the weighted average data from the laser-based measurements from NCU and NIST. Upon comparison of all measured line intensities, there is no evidence of substantial (much greater than 1‰) systematic deviation about the reference UCL values. This demonstrated consistency in measured intensities puts an upper bound on any unaccounted-for systematic bias in the three sets of measurements performed using the three different experimental techniques considered here.

We present both literature (closed symbols) intensities and our experimental values (open symbols) relative to our theoretical values in Fig. 1(c). In contrast to the other panels in Fig. 1, note the significantly extended range along the y axis. The scatter and the m-dependent structure of the literature data about the theoretical intensities are more than an order of magnitude greater than those of our measured values, which are nearly indistinguishable from zero on the chosen scale. We reemphasize that the mutual agreement with theory of our laser-based and FTS spectroscopic line intensity measurements (both of which are Système International traceable and can be considered as primary measurements of line intensity) is unprecedented. These measurements span a sufficiently broad range of rotational quanta to confirm both the calculated J dependence (band shape) of the component intensities as well as the total band intensity (given below). Combining the present results from all three experimental techniques and all lines yields an average deviation between experiment and theory of 0.6‰ with a standard deviation of 0.9‰, representing a more than order-of-magnitude improvement in measurement precision and accuracy compared to the literature values given in Fig. 1(c). We note that, with the exception of Ref. [36], all the literature data presented were acquired with the FTS technique. The relatively high precision and accuracy achieved with the present FTS measurements are ascribed to several factors, including precise temperature stabilization, characterization of the sample path length and instrument line shape function, single-polynomial fits to the baseline, high signal-to-noise ratio (nominally 2000∶1), and the use of an InGaAs detector with high linearity.

In Fig. 1(d), we also compare the present experimental and theoretical results to the HITRAN 2020 [42] intensities for the (3–0) band of $^{12}C^{16}O$. The latter intensities are based on a semiempirical dipole-moment function that is determined by global fitting to measured intensities from multiple vibrational bands of this molecule. Comparison of our theoretical intensities (see Fig. 1(d) and SM)

TABLE I. Comparison of experimental (NCU, NIST, and PTB) and calculated line intensities in the (3–0) of CO. Reported intensities, S, are based on the reference temperature $T = 296$ K, and scaled to 100% relative abundance of the $^{12}C^{16}O$ isotopologue. Intensity units are in $cm^2\,cm^{-1}$/molecule. Line wave numbers are from HITRAN 2020 [42].

Line $\bar{\nu}$ (cm^{-1})	S_{NIST} (cm/molecule)	S_{NCU} (cm/molecule)	S_{PTB} (cm/molecule)	$S_{NIST}/S_{UCL} - 1$ (‰)	$S_{NCU}/S_{UCL} - 1$ (‰)	$S_{PTB}/S_{UCL} - 1$ (‰)
P30 6190.07	1.5790(28)E-26	1.5758(18)E-26		3.3	1.3	
P27 6210.25	7.3680(120)E-26	7.3608(76)E-26		−0.8	−1.7	
P27 6210.25	7.3658(82)E-26[a]			−1.0		
P20 6253.78			1.3514(18)E-24			2.3
P15 6281.82			5.7460(75)E-24			1.2
P10 6307.29			1.3675(18)E-23			1.2
P5 6330.17			1.5321(20)E-23			0.5
R5 6371.30			2.1075(28)E-23			0.6
R10 6385.77			1.9505(26)E-23			0.7
R15 6397.58			8.989(12)E-24			0.5
R20 6406.70			2.3469(31)E-24			−1.1
R23 6410.88	8.1687(74)E-25	8.1719(77)E-25		0.3	0.7	
R23 6410.88		8.1659(58)E-25[b]			−0.1	
R26 6414.08	2.3661(33)E-25	2.3668(24)E-25		−0.1	0.2	
R27 6414.93	1.5034(21)E-25	1.5049(16)E-25		−1.0	0.0	
R28 6415.67	9.397(18)E-26	9.386(11)E-26		1.4	0.3	
R29 6416.30	5.7300(94)E-26	5.7371(63)E-26		−1.4	−0.2	

[a]Measurement conducted at NIST in 2018.
[b]Measurement conducted at NCU in 2019 [3].

with those from HITRAN 2020 reveals a nearly quadratic trend with rotational quantum number. This quantity is about 5‰ near band center and exhibits a slope of nominally −0.2‰. In addition to this discrepancy in the rotational dependence of line intensity, the HITRAN 2020 band intensity (based on summing over lines P46 to R48) is about 4.6‰ smaller than our theoretical value of 4.7361×10^{-22} cm^2 cm^{-1}/molecule.

We also compare our results to a semiempirical line list for CO (see Fig. 1(d); blue stars) that has recently been created. Similar to generation of the HITRAN 2020 line list, the new one was based on a global fit of a parametrized DMC to multiple CO vibrational bands (up to the fifth overtone) [41]. Comparison to our results shows good agreement (at the promille level) both with the present experimental data and *ab initio* calculations. However, the two sets of calculated values tend to diverge with increasing J in the P branch, with differences of 2.0‰ at $m = -25$ that increase to 3.7‰ at $m = -46$. Thus, our comparison between the present *ab initio* intensities and the semi-empirical results from [41] also provides a measure of uncertainty in the latter values, which without the present results cannot be easily assessed. This difficulty arises because uncertainties in the intensity data from prior measurements, which were used in the global fit of [41], are often underestimated, as can be seen in Fig. 1(c). For example, it would have been difficult to identify the systematic offset in the P branch (at the promille level) without reference to the present results.

Our theoretical model should reliably predict intensities for all vibrational bands of CO. Unfortunately, experimental results with sufficient precision and accuracy (such as those demonstrated here for the (3–0) band) needed to validate this predictive capability in the other CO bands at the subpromille level do not exist. Notwithstanding this limitation, we can say that for the (1-0), (2–0), and (4–0) bands, our new model for CO intensities is consistent with other experimental results in the literature within their reported percent-level uncertainties (see SM [28–33,44,45]). Our theoretical line intensities for these bands are given in Tables II–V of the SM. Higher overtones, including the (5–0) band and beyond, will require additional work because the calculated intensities are affected not only by the accuracy of the quantum chemistry calculations, but also by that of the DMC functional form [46].

We propose that the present theoretical (3–0) CO line intensities could be used as intrinsic spectroscopic references to improve measurement accuracy in the case of techniques such as FTS and cavity-enhanced spectroscopy [47] that require knowledge of the optical path length (see SM for details). For cases of comparable optical thickness and line shape in both the reference and unknown spectra, this approach could help reduce biases in retrieved absorber number density that depend on signal-to-noise ratio and are driven by nonlinear dependence of the spectrum on absorber number density. This approach would be nearly cost-free and has the potential to reduce systematic relative

uncertainties toward promille levels in the case of long-path spectrometers.

---

[*]Corresponding author.
j.tennyson@ucl.ac.uk

[1] Z. D. Reed, D. A. Long, H. Fleurbaey, and J. T. Hodges, Optica **7**, 1209 (2020).

[2] D. Lisak, D. K. Havey, and J. T. Hodges, Phys. Rev. A **79**, 052507 (2009).

[3] A. Cygan, P. Wcisło, S. Wójtewicz, G. Kowzan, M. Zaborowski, D. Charczun, K. Bielska, R. S. Trawiński, R. Ciuryło, P. Masłowski *et al.*, Opt. Express **27**, 21810 (2019).

[4] A. J. Fleisher, E. M. Adkins, Z. D. Reed, H. Yi, D. A. Long, H. M. Fleurbaey, and J. T. Hodges, Phys. Rev. Lett. **123**, 043001 (2019).

[5] D. A. Long, Z. D. Reed, A. J. Fleisher, J. Mendonca, S. Roche, and J. T. Hodges, Geophys. Res. Lett. **47**, e2019GL086344 (2020).

[6] M. Birk, C. Röske, and G. Wagner, J. Quant. Spectrosc. Radiat. Transfer **272**, 107791 (2021).

[7] M. P. Arroyo and R. K. Hanson, Appl. Opt. **32**, 6104 (1993).

[8] R. Wehr, E. McKernan, A. Vitcu, R. Ciurylo, and J. R. Drummond, Appl. Opt. **42**, 6595 (2003).

[9] C. Gaiser, B. Fellmuth, and W. Sabuga, Nat. Phys. **16**, 177 (2020).

[10] A. J. Fleisher, H. Yi, A. Srivastava, O. L. Polyansky, N. F. Zobov, and J. T. Hodges, Nat. Phys. **17**, 889 (2021).

[11] O. L. Polyansky, K. Bielska, M. Ghysels, L. Lodi, N. F. Zobov, J. T. Hodges, and J. Tennyson, Phys. Rev. Lett. **114**, 243001 (2015).

[12] I. E. Gordon, L. S. Rothman, C. Hill, R. V. Kochanov, Y. Tan, P. F. Bernath, M. Birk, V. Boudon, A. Campargue, K. V. Chance *et al.*, J. Quant. Spectrosc. Radiat. Transfer **203**, 3 (2017).

[13] A. Cygan, P. Wcisło, S. Wójtewicz, P. Masłowski, J. T. Hodges, R. Ciuryło, and D. Lisak, Opt. Express **23**, 14472 (2015).

[14] H. Lin, Z. D. Reed, V. T. Sironneau, and J. T. Hodges, J. Quant. Spectrosc. Radiat. Transfer **161**, 11 (2015).

[15] Z. D. Reed, D. A. Long, H. Fleurbaey, and J. T. Hodges, Optica **7**, 1209 (2020).

[16] K. Lehmann, in *Cavity Ring-Down Spectroscopy*, edited by K. Busch and M. Busch (American Chemical Society, Washington DC, 1999), pp. 106–124.

[17] V. Werwein, J. Brunzendorf, G. Li, A. Serdyukov, O. Werhahn, and V. Ebert, Appl. Opt. **56**, E99 (2017).

[18] N. H. Ngo, D. Lisak, H. Tran, and J.-M. Hartmann, J. Quant. Spectrosc. Radiat. Transfer **129**, 89 (2013).

[19] A. S. Pine and R. Ciuryło, J. Mol. Spectrosc. **208**, 180 (2001).

[20] See Supplemental Material, which includes Refs. [21–33], at http://link.aps.org/supplemental/10.1103/PhysRevLett.129.043002 for details of experimental and theoretical procedures used plus full numerical intensity results for the fundamental and first three overtone bands of $^{12}C^{16}O$.

[21] G.-W. Truong, K. O. Douglass, S. E. Maxwell, R. D. van Zee, D. F. Plusquellic, J. T. Hodges, and D. A. Long, Nat. Photonics **7**, 532 (2013).

[22] J. H. Hendricks and D. A. Olson, Measurement **43**, 664 (2010), ISSN 0263-2241, iMEKO XIX World Congress Part 1 Advances.

[23] M. Konefał, M. Słowiński, M. Zaborowski, R. Ciuryło, D. Lisak, and P. Wcisło, J. Quant. Spectrosc. Radiat. Transfer **242**, 106784 (2020).

[24] I. I. Mizus, L. Lodi, J. Tennyson, N. F. Zobov, and O. L. Polyansky, J. Mol. Spectrosc. **386**, 111621 (2022).

[25] S. N. Yurchenko, L. Lodi, J. Tennyson, and A. V. Stolyarov, Comput. Phys. Commun. **202**, 262 (2016).

[26] K. A. Peterson and T. H. Dunning, J. Chem. Phys. **117**, 10548 (2002).

[27] L. Lodi, J. Tennyson, and O. L. Polyansky, J. Chem. Phys. **135**, 034113 (2011).

[28] J. M. Hartmann, M. Y. Perrin, J. Taine, and L. Rosenmann, J. Quant. Spectrosc. Radiat. Transfer **35**, 357 (1986).

[29] V. C. Devi, D. C. Benner, K. Sung, T. J. Crawford, G. Li, R. R. Gamache, M. A. H. Smith, I. E. Gordon, and A. W. Mantz, J. Quant. Spectrosc. Radiat. Transfer **218**, 203 (2018).

[30] Q. Zou and P. Varanasi, J. Quant. Spectrosc. Radiat. Transfer **75**, 63 (2002).

[31] P. Varanasi and S. Sarangi, J. Quant. Spectrosc. Radiat. Transfer **15**, 473 (1975).

[32] K. Sung and P. Varanasi, J. Quant. Spectrosc. Radiat. Transfer **91**, 319 (2005).

[33] L. Régalia-Jarlot, X. Thomas, P. Von der Heyden, and A. Barbe, J. Quant. Spectrosc. Radiat. Transfer **91**, 121 (2005).

[34] J. A. Coxon and P. G. Hajigeorgiou, J. Chem. Phys. **121**, 2992 (2004).

[35] H.-J. Werner, P. J. Knowles, F. R. Manby, J. A. Black, K. Doll, A. Heßelmann, D. Kats, A. Köhn, T. Korona, D. A. Kreplin *et al.*, J. Chem. Phys. **152**, 144107 (2020).

[36] J. Henningsen, H. Simonsen, T. Mogelberg, and E. Trudso, J. Mol. Spectrosc. **193**, 354 (1999).

[37] D. Jacquemart, J. Y. Mandin, V. Dana, N. Picqué, and G. Guelachvili, Eur. Phys. J. D **14**, 55 (2001).

[38] C. Chackerian, R. Freedman, L. P. Giver, and L. R. Brown, J. Mol. Spectrosc. **210**, 119 (2001).

[39] K. Y. Sung and P. Varanasi, J. Quant. Spectrosc. Radiat. Transfer **83**, 445 (2004).

[40] Y. G. Borkov, A. M. Solodov, A. A. Solodov, T. M. Petrova, E. V. Karlovets, and V. I. Perevalov, J. Quant. Spectrosc. Radiat. Transfer **253**, 107064 (2020).

[41] V. V. Meshkov, A. Y. Ermilov, A. V. Stolyarov, E. S. Medvedev, V. G. Ushakov, and I. E. Gordon, J. Quant. Spectrosc. Radiat. Transfer **280**, 108090 (2022).

[42] I. E. Gordon, L. S. Rothman, R. J. Hargreaves, R. Hashemi, E. V. Karlovets, F. M. Skinner, E. K. Conway, C. Hill, R. V. Kochanov, Y. Tan *et al.*, J. Quant. Spectrosc. Radiat. Transfer **277**, 107949 (2022).

[43] A. Cygan, A. J. Fleisher, R. Ciuryło, K. A. Gillis, J. T. Hodges, and D. Lisak, Commun. Phys. **4**, 14 (2021).

[44] G. Li, I. E. Gordon, L. S. Rothman, Y. Tan, S.-M. Hu, S. Kassi, A. Campargue, and E. S. Medvedev, Astrophys. J. Suppl. Ser. **216**, 15 (2015).

[45] V. Malathy Devi, D. Chris Benner, M. A. H. Smith, A. W. Mantz, K. Sung, L. R. Brown, and A. Predoi-Cross, J. Quant. Spectrosc. Radiat. Transfer **113**, 1013 (2012).

[46] E. S. Medvedev and V. G. Ushakov, J. Quant. Spectrosc. Radiat. Transfer **272**, 107803 (2021).

[47] L. Gianfrani, R. W. Fox, and L. Hollberg, J. Opt. Soc. Am. B **16**, 2247 (1999).